DOI: 10.1002/chem.201000717

Structure–Function Relationships in Liquid-Crystalline Halogen-Bonded Complexes

Duncan W. Bruce,*[a] Pierangelo Metrangolo,*[b] Franck Meyer,[b] Tullio Pilati,[c] Carsten Präsang,[a] Giuseppe Resnati,*[b] Giancarlo Terraneo,[b] Stephen G. Wainwright,[a] and Adrian C. Whitwood[a]

Abstract: New liquid-crystalline materials were prepared by self-assembly driven by halogen bonding between a range of 4-alkoxystilbazoles, 4-alkyl-, and 4-alkoxy-substituted pyridines as halogen-bonding acceptors, and substituted derivatives of 4-iodotetrafluorophenyl as halogen-bonding donors. Despite the fact that the starting materials are not mesomorphic, the dimeric, halogen-bonded complexes obtained exhibited nematic and SmA phases, depending on the length of the alkyl chains present on the components. The modularity of this approach also led to new chiral mesogens starting from non-mesomorphic chiral compounds.

Keywords: fluorinated mesogens · halogen bonding · liquid crystals · self-assembly · supramolecular chemistry

Introduction

In addition to their ubiquity in flat-panel display devices, liquid crystals are increasingly attracting attention as materials with actual and postulated application in fields as diverse as biotechnology, nanoscience, and several other classes of advanced optical materials.[1] Such advances are based primarily on covalent materials, but the attractions of constructing new species from non-covalent interactions have led many in the field to explore the generation of new mesogenic species using, for example, hydrogen-bonding, charge-transfer, and quadrupolar interactions.[2]

As a counterpart of hydrogen bonding, halogen bonding is emerging in the field of crystal engineering and supramolecular chemistry in general.[3] It is commonly established that halogen bonding concerns any non-covalent interaction involving a halogen atom as an acceptor of electronic density.[3e,4]

This topic has ensured the construction of supramolecular architectures in fields of research as diverse as solid state synthesis,[5] nonlinear optics,[6] polymer coatings,[7] separation technologies,[8] and the formation of highly interpenetrated networks.[9]

Recently, halogen bonding has been shown to be useful in the realisation of new liquid-crystalline materials assembled from non-mesomorphic components.[10] Subsequent investigations pursued the design and synthesis of halogen-bonded liquid crystals in polymeric systems[11] and in trimeric complexes,[12] one example of which led to spontaneous resolution into chiral forms despite the absence of chirality in the complexes themselves.[13] However, all of this work reports the mesomorphism of a quite diverse selection of halogen-bonded mesogens, which means that there is little chance for systematic structural comparison. More than that, rather few of the low molar mass systems reported have enantiotropic mesophases and none possesses a chiral function.

In many different topics, fluorinated compounds present an enhancement of physical properties in contrast with their hydrocarbon homologues.[14] As expected, fluorinated sub-

[a] Prof. Dr. D. W. Bruce, Dr. C. Präsang, S. G. Wainwright, Dr. A. C. Whitwood
Department of Chemistry, University of York
Heslington, York YO10 5DD (UK)
Fax: (+44) 1904-432516
E-mail: db519@york.ac.uk

[b] Prof. Dr. P. Metrangolo, Dr. F. Meyer, Prof. Dr. G. Resnati, Dr. G. Terraneo
NFMLab and CNST-IIT@POLIMI c/o Department of Chemistry
Materials, and Chemical Engineering "Giulio Natta"
Politecnico di Milano 7, via Mancinelli; 20131 Milan (Italy)
Fax: (+39) 02-2399-3080
E-mail: pierangelo.metrangolo@polimi.it
giuseppe.resnati@polimi.it

[c] Dr. T. Pilati
CNR—Institute of Molecular Science and Technology
University of Milan 19, via Golgi; 20133 Milan (Italy)

Supporting information for this article is available on the WWW under http://dx.doi.org/10.1002/chem.201000717.

stituents have been incorporated successfully into liquid-crystal compounds because of the combination of high polarity and small size, and because the high strength of the C–F bond confers excellent chemical stability.[15] However, significant modifications are encountered frequently in respect of transitions temperatures, melting points, mesophase morphologies, and the many essential physical properties of liquid crystals, such as visco-elastic, dielectric, and optical responses. Moreover, fluorination has also been demonstrated to be a driving force in molecular recognition, and microphase separation between perfluorocarbon and hydrocarbon chains has led to control over the liquid-crystalline phases a mesogen exhibits. Thus, the covalent incorporation of perfluorocarbon chains into mesogens will induce a microphase separation as a result of the fluorophobic effect.[16] In general, this feature gives rise to the effective absence of nematic phases and the enhancement of the smectic character of a mesomorphic material.[17]

In the present study, therefore, we have undertaken an investigation in which we have prepared a number of supramolecular halogen-bonded mesogens and have varied the structures systematically to provide new insights into these materials. The basis for these new materials is a 4-substituted pyridine, in most cases an alkoxystilbazole (halogen-bonding acceptor) and a 4-substituted iodotetrafluorobenzene (halogen-bonding donor) as shown in Scheme 1, and we have varied the total number of aromatic rings and their disposition, as well as the length and nature of the terminal chains. The formation and mesomorphism of these dimeric systems is now described in detail.

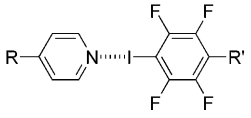

Scheme 1. General dimeric halogen-bonded liquid-crystalline materials.

Results and Discussion

Synthesis: Alkoxystilbazoles[18] (**1**-*m* in which *m* is the number of carbon atoms in the terminal alkoxy chain) have been shown to be versatile starting units for the design of functional materials and more particularly liquid-crystalline compounds,[19] and so they formed the basis for the majority of halogen-bonding acceptors used in this study. The other Lewis bases (Scheme 2) used were 4-octylpyridine (**7**) and 4-octyloxypyridine (**8**),[20] both well-known compounds. On the other hand, several, related families of iodotetrafluorobenzene derivatives were employed in this study as new halogen-bonding donors, the synthesis of which is now described (Scheme 3).

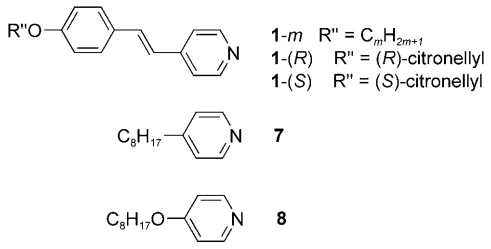

Scheme 2. The families of nitrogen bases (**1**-*m*, **7**, and **8**) used in this study.

The partially fluorinated stilbene compounds **2** were obtained by a Wittig reaction between 4-alkoxybenzaldehyde and the phosphonium salt of 4-*H*-tetrafluorobenzyl bromide. Alkylation of 4-hydroxybenzaldehyde with the appropriate iodoalkane was carried out in acetone under reflux in the presence of K_2CO_3. For the chiral compounds, *(S)*- and *(R)*-citronellyl were chosen as the chains for the alkylation of 4-hydroxybenzaldehyde. Finally, the iodination reactions of the 4-*H*-tetrafluorophenyl rings were carried out by using BuLi/I_2 in dry THF, affording compounds **2** in good yield.

The key intermediate in the preparation of **3**-*n* was 4-iodotetrafluorophenol, which was obtained by nucleophilic substitution of iodopentafluorobenzene by using OH^-. The final ester was prepared using standard dicyclohexyl carbodiimide/4-dimethylaminopyridine (DCC/DMAP) conditions. The more highly fluorinated esters, **4**-*n*, required the use of 4-alkoxytetrafluorobenzoic acid, which was obtained from alkoxy-2,3,5,6-tetrafluorobenzene (itself obtained by *O*-alkylation of 2,3,5,6-tetrafluorophenol) by lithiation (BuLi) and then bubbling CO_2 through the solution. Reversed esters **5**-*n* were prepared by esterification of 4-iodo-2,3,5,6-tetrafluorobenzoic acid with a 4-alkoxyphenol. The iodobenzoic acid was prepared from pentafluorobenzoic acid by removing the *para*-fluorine using Zn in aqueous ammonia and then iodinating the 2,3,4,5-tetrafluorobenzoic acid so produced using BuLi/I_2. Finally, compounds **6**-*n* were prepared by using Williamson ether procedures to *O*-alkylate the phenol before introducing the iodine using BuLi and I_2 (see Supporting Information for the synthetic details).

Crystal and molecular Structure of 1-10·2-6 and 1-6·6-6: The halogen-bonded complex **1**-10·**2**-6 (Scheme 4) was crystallised by mixing equimolar amounts of stilbazole **1**-10 and fluorinated stilbene **2**-6 in THF, leading to the formation of the dimeric species as illustrated. Slow evaporation of the solvent at room temperature after two days yielded good quality needle-like single crystals of **1**-10·**2**-6 suitable for X-ray diffraction. The halogen-bonded dimers found in the crystal structure of **1**-10·**2**-6 are illustrated in Figure 1 and crystallographic data are reported in Table 1.

The supramolecular dimers in **1**-10·**2**-6 are linked by N···I halogen bonds with a distance of 2.798(2) Å, which corresponds to a reduction of approximately 21% of the sum of van der Waals' radii for N and I (3.53 Å) (Figure 1).[21] The N···I–C angle is almost linear (178.81(7)°).[22] Moreover, all four phenyl rings of the dimer are coplanar and the alkyl chains adopt a perfect *all-trans* linear arrangement and are coplanar with the phenyl rings. Through a centre of symmetry, two different dimers are held together in an antiparallel fashion in the plane of the aromatic rings by intermolecular H···F contacts (2.49 Å), involving the hydrogen atoms of the

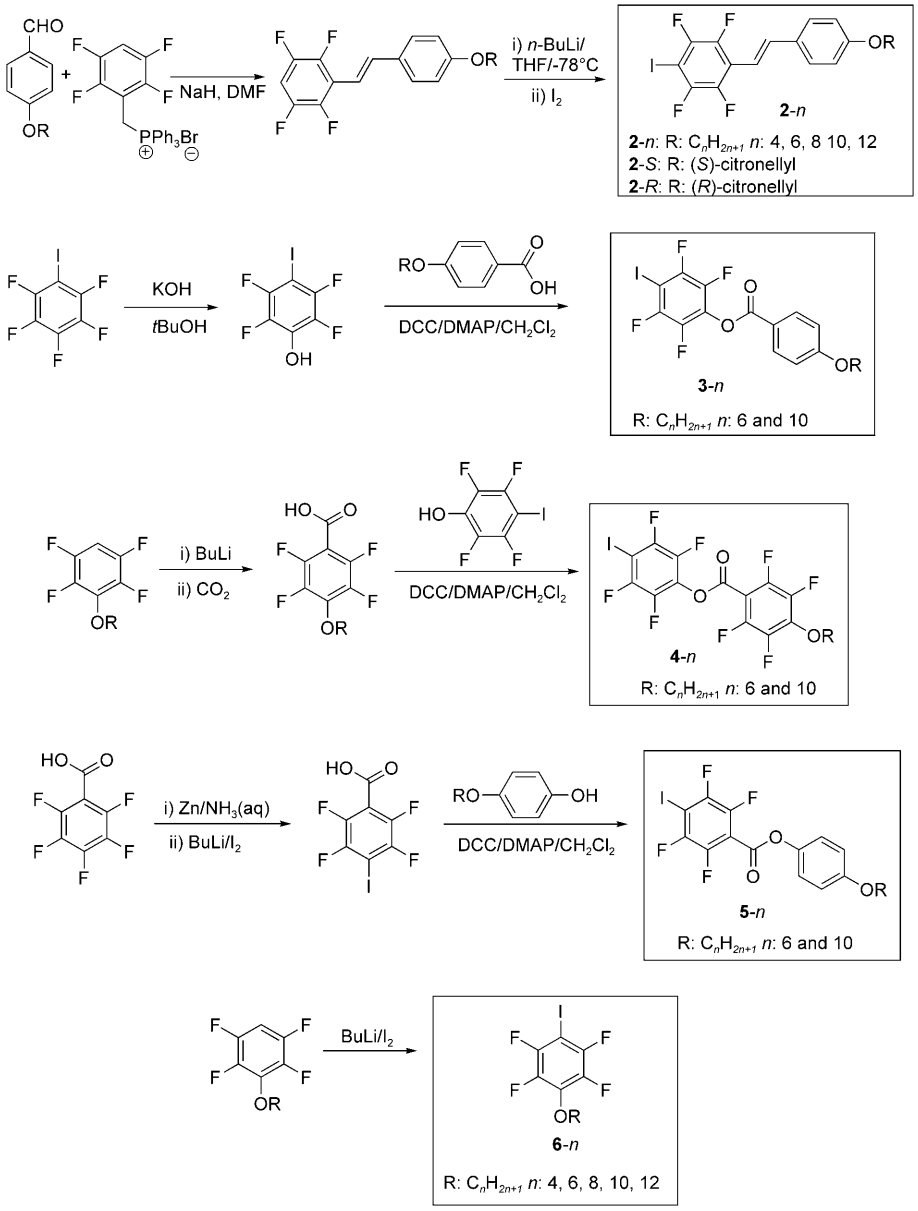

Scheme 3. Preparation of the iodo compounds used in this study.

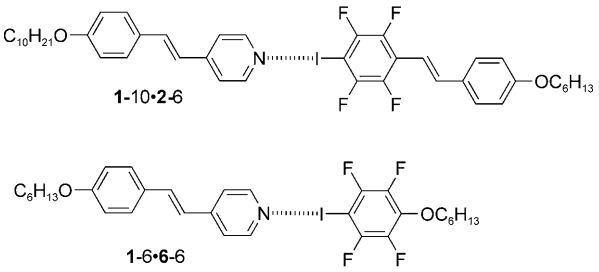

Scheme 4. General structures of **1**-10·**2**-6 and **1**-6·**6**-6.

pyridyl ring of **2**-6. This leads to the formation of supramolecular tetramers that are now packed in an infinite ribbon thanks to other intermolecular H···F contacts (of about 2.57 Å) between antiparallel molecules of **2**-6.[23] These ribbons are packed together only by residual forces.

The complex **1**-6·**6**-6 (Scheme 4) was similarly crystallised from THF giving rise to very thin, colourless plate-like crystals of poor quality, which were, however, submitted to single-crystal X-ray diffraction and a structure solved. The two independent, halogen-bonded dimers found in the crystal structure of **1**-6·**6**-6 are illustrated in Figure 2 and crystallographic data are reported in Table 1.

The structures of the two dimers in **1**-6·**6**-6 are quite different from each other and from the one seen in **1**-10·**2**-6. In fact, the mean-square planes of the stilbazole rings in **1**-6·**6**-6 are rotated with respect to those of the halogen-bonded modules **6**-6 by 31.1 and 13.1°, while in **1**-10·**2**-6 the same angle is 8.6°. Moreover, both in **1**-6 and in **6**-6 the alkoxy chains are not coplanar with the aromatic rings, as seen in **1**-10·**2**-6. In particular, the dihedral angles for **1**-6 are 44.5° and 46.1°, while the same angle for **1**-10 is 1.9°; also the conformations of the alkoxy chains are different, being *gttt* and *tgtt* in **1**-6 and *tttt* in **1**-10. In **6**-6 the dihedral

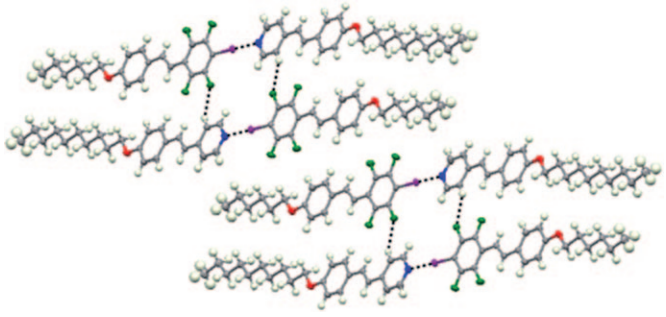

Figure 1. The halogen-bonded dimeric complex **1**-10·**2**-6 forming planar ribbons. Colours are as follows: C, grey; H, white; F, green; I, purple; N, blue; O, red. Halogen bonds contacts are shown by dotted black lines. Ellipsoids drawn at the 20% probability level and non-covalent interactions are selecetd to be shorter than the sum of the van der Walls' radii less 0.1 Å.

Table 1. Crystal data and structure refinement for the halogen-bonded dimeric complexes **1**-10·**2**-6 and **1**-6·**6**-6.

	1-10·**2**-6	**1**-6·**6**-6
formula	$C_{23}H_{31}NO{\cdot}C_{20}H_{19}F_4IO$	$C_{19}H_{23}NO{\cdot}C_{12}H_{13}F_4IO$
M_r [g mol^{-1}]	815.74	657.51
crystal size [mm^3]	0.12×0.15×0.48	0.02×0.14×0.22
crystal system	triclinic	triclinic
space group	$P\bar{1}$ (no. 2)	$P\bar{1}$ (no. 2)
a [Å]	6.0015(12)	9.5019(11)
b [Å]	15.906(3)	12.7799(14)
c [Å]	21.269(5)	24.939(3)
α [°]	78.082(10)	85.107(2)
β [°]	84.652(10)	79.141(2)
γ [°]	88.812(10)	86.225(2)
V [Å^3]	1977.9(7)	2959.5(6)
Z	2	4
ρ_{calcd} [g cm^{-3}]	1.370	1.476
$F(000)$	840	1336
T [K]	295(2)	110(2)
θ_{max} [°]	26.41	25.04
index ranges	$-7\le h\le 7$	$-11\le h\le 11$
	$-19\le k\le 19$	$-15\le k\le 15$
	$-26\le l\le 26$	$-29\le l\le 29$
reflns measured	8135	6597
observed reflns	28132 [$I_o \ge 2\sigma(I_o)$]	23757 [$I_o \ge 2\sigma(I_o)$]
independent reflns	8135 (R_{int}=0.0254)	10409 (R_{int}=0.0891)
final R indices[a]	R_1=0.0265	R_1=0.0727
(obs. data)	wR_2=0.0595	wR_2=0.1773
S[b]	1.034	0.962
Max/av Δ/σ	0.001/0.000	0.000/0.000
$\Delta\rho_{min/max}$ [e Å^{-3}]	−0.23/0.42	−2.44/2.55

[a] $R_1=\Sigma||F_o|-|F_c||/\Sigma|F_o|$, $wR_2=[\Sigma w(F_o^2-F_c^2)^2/\Sigma wF_o^4]^{1/2}$. [b] Goodness-of-fit $S=[\Sigma w(F_o^2-F_c^2)^2/(n-p)]^{1/2}$, in which n is the number of reflections and p the number of parameters.

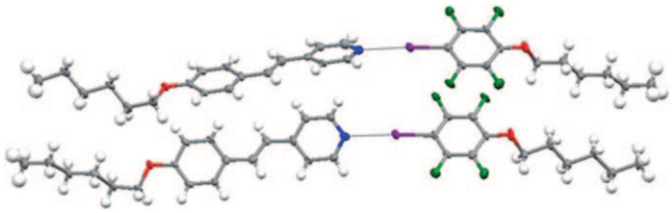

Figure 2. The two asymmetric dimers in the crystal structure of the halogen-bonded complex **1**-6·**6**-6. Colours are as follow: C, grey; H, white; F, green; I, purple; N, blue; O, red. Halogen bonds are dotted blue lines.

angles are 89.7 and 52.4°, while in **1**-10·**2**-6 the alkoxy chains are almost coplanar with the aromatic rings of **2**-6, the angle being 2.4°. This difference is probably due to the steric hindrance present in **6**-6 between the hydrogen atoms of the $^-O-CH_2^-$ group and the F atoms in the *ortho*-position of the tetrafluorophenyl ring.

Mesomorphic properties of the complexes: Having obtained the stilbazoles (**1**-*m*), pyridines (**7** and **8**) and the various iodotetrafluobenzenes (**2**-*n* to **6**-*n*), several series of halogen-bonded complexes were prepared to evaluate their liquid-crystal properties. In almost every case, the complexes were prepared by co-crystallisation from THF and the mesomorphism reported is that of the crystalline material so obtained. However, not every donor–acceptor pairing behaved well and so for some materials it was not possible to obtain crystalline materials in this way. In these cases (which will be discussed below), the complexes were prepared by weighing out equimolar quantities of the two components very carefully and mixing them together in the melt. Some of us have used such a procedure before in preparing hydrogen-bonded liquid-crystalline materials and found it to be a satisfactory procedure—indeed on many occasions it was absolutely necessary, for example, if one components was rather insoluble.[24] In the present work, the efficacy of this approach was tested by preparing complexes in the melt for pairings for which crystallisation was also successful. The differences will be outlined below. Two extensive series of related materials were first prepared to examine structure/mesomorphism relationships in detail and then some representative examples were prepared using a slightly wider range of iodides or the alkyl(oxy)pyridines. It should be noted that none of the components was liquid crystalline and so all mesomorphic properties arise from halogen-bonded dimers (the possibility that quadrupolar arene/perfluoroarene interactions were involved was discounted previously on the basis of experimental evidence).[10]

Complexes with achiral stilbenes 2-*n*: Systematic crystallisation of **1**-*m* with **2**-*n* ($n=m=4$, 6, 8, 10, 12) produced twenty-five dimers (Scheme 5; Table 2), the thermal behaviour of which was evaluated by using polarised optical microscopy and differential scanning calorimetry (DSC); the results are collected in Table 3. Melting points are typically in the range 99.3–119.1 °C and clearing points are in the range 108.5–130.4 °C, giving an average range of 9 °C.

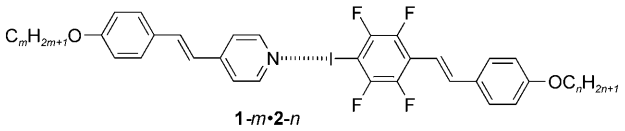

1-*m*•**2**-*n*

Scheme 5. General structure for complexes **1**-*m*·**2**-*n*.

Table 2. Observed phases in 5×5 square matrix: parentheses indicate a monotropic phase.

2-*n*/**1**-*m*	**1**-4	**1**-6	**1**-8	**1**-10	**1**-12
2-4	N, (SmA)	N	N	N	N, (SmA)
2-6	N	N	N	N	N, (SmA)
2-8	N	N	N	N, (SmA)	N, (SmA)
2-10	N	N	N	N, (SmA)	N, SmA
2-12	N	N	N	N, (SmA)	N, SmA

The thermal data were first analysed with respect to a fixed chain length for the stilbene. Thus, the typical feature of compounds **1**-6·**2**-4 to **1**-12·**2**-4 was an enantiotropic nematic phase with a range between 9.1 to 13.3 °C, the phase being identified clearly by its schlieren texture (Figure 3, left). Figure 4 shows these transition temperatures and those for **1**-*m*·**2**-6 and reveals a monotonic destabilisation of the

Table 3. Thermal data for complexes **1**-*m*·**2**-*n*.

	Transition[a]	T [°C]	ΔH [kJ mol^{-1}]
1-4·**2**-4	Cr–N	119.4	19.8
	N–I	130.3	2.1
	(SmA–N)	(116.4)	(0.3)
1-6·**2**-4	Cr–N	114.5	50.9
	N–I	123.5	7.6
1-8·**2**-4	Cr–N	109.5	27.1
	N–I	122.6	2.9
1-10·**2**-4	Cr–N	104.2	15.2
	N–I	117.5	1.4
1-12·**2**-4	Cr–N	104.3	65.9
	N–I	114.2	4.6
	(SmA–N)	(93.5)	–
1-4·**2**-6	Cr–N	115.8	55.6
	N–I	125.5	6.6
1-6·**2**-6	Cr–N	114.2	36.8
	N–I	121.5	3.5
1-8·**2**-6	Cr–N	107.3	8.8
	N–I	116.8	0.8
1-10·**2**-6	Cr–N	105.9	52.5
	N–I	116.1	4.91
1-12·**2**-6	Cr–N	105.4	43.4
	N–I	111.7	3.8
	(N–SmA)	(108.3)	–
1-4·**2**-8	Cr–N	109.4	75.1
	N–I	120.8	8.7
1-6·**2**-8	Cr–N	107.1	36.9
	N–I	116.3	5.4
1-8·**2**-8	Cr–N	104.4	40.8
	N–I	114.6	2.9
1-10·**2**-8	Cr–N	104.4	22.9
	N–I	112.5	1.3
	(SmA-N)	(87.2)	(0.4)
1-12·**2**-8	Cr–N	102.9	21.8
	N–I	111.3	3.0
	(SmA-N)	(99.8)	(0.3)
1-4·**2**-10	Cr–N	110.4	29.6
	N–I	117.5	3.3
1-6·**2**-**1**0	Cr–N	106.5	46.1
	N–I	117.3	4.8
1-8·**2**-10	Cr–N	103.9	34.0
	N–I	113.6	4.4
1-10·**2**-10	Cr–N	103.2	46.6
	N–I	112.3	5.3
	(SmA–N)	(95.4)	(0.2)
1-12·**2**-10	Cr–N	103.0	56.3
	SmA–N	105.0	0.5
	N–I	110.2	7.7
1-4·**2**-12	Cr–N	109.5	31.8
	N–I	111.8	1.9
1-6·**2**-12	Cr–N	108.0	41.4
	N–I	110.0	4.4
1-8·**2**-12	Cr–N	107.3	39.2
	N–I	109.0	5.3
1-**1**0·**2**-12	Cr–N	105.1	41.3
	N–I	108.5	5.1
	(SmA–N)	(100.0)	(0.1)
1-12·**2**-12	Cr–N	106.0	66.3
	SmA–N	108.6	0.7
	N–I	111.1	4.9

[a] Where a monotropic transition is written in heating sequence, it means that it was possible to obtain transition the temperature (and enthalpy where given) on reheating, giving the true thermodynamic temperature.

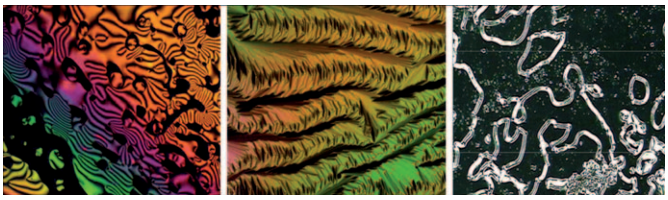

Figure 3. Left: nematic phase of **1**-4·**2**-4; middle: smectic A phase of **1**-4·**2**-4; right: mainly homeotropic SmA phase of **1**-10·**2**-8.

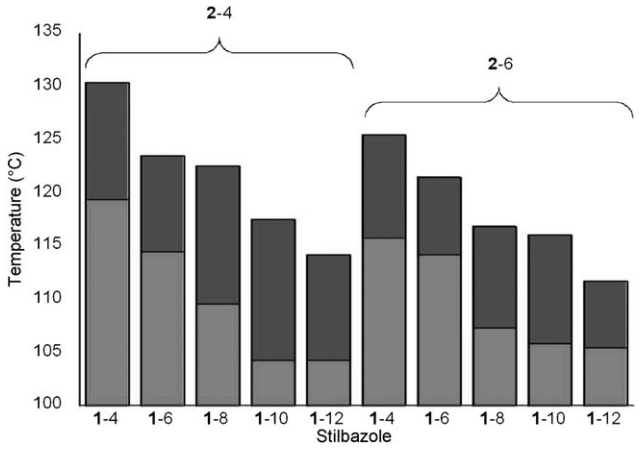

Figure 4. Chart of the thermal behaviour of complexes **1**-*m*·**2**-4 and **1**-*m*·**2**-6 (light grey is the crystal phase; dark grey is nematic).

nematic phase with increasing *m*, which is common behaviour in calamitic mesogens with two terminal chains. A similar picture emerges when considering the variation of the stilbene chain length for other stilbazoles.

It is similarly possible to consider the data for a fixed chain length for the stilbazole, and Figure SI-1 (see Supporting Information) shows a similar monotonic decrease in T_{N-I} as a function of the stilbene chain length for **1**-4·**2**-4 to **1**-4·**2**-12 and **1**-6·**2**-4 to **1**-6·**2**-12.

However, what Figure 4 and Figure SI-1 do not show is that for the longest stilbazole chain lengths (and for **1**-4·**2**-4; Figure 3 middle), there is also a monotropic SmA phase, and for stilbenes **2**-8, **2**-10 and **2**-12 the monotropic SmA phase is also seen for **1**-10 until at **1**-12·**2**-12 it appears enantiotropically; the evolution of this behaviour is illustrated in Figure 4. All of this is consistent with the conventional view that increasing the terminal chain length stabilises the formation of layered phases, and the fact that a monotropic SmA phase is seen in complex **1**-4·**2**-4, suggests the latent existence of the phase in all of the complexes studied.

The complexes reported here are of some interest as they represent the first series of halogen-bonded mesogens in which the predominant mesomorphism is enantiotropic. This point will be discussed below.

Complexes with chiral stilbazoles 1-(*R*) and 1-(*S*) and chiral stilbenes 2-(*R*) and 2-(*S*): Having demonstrated mesomorphism in achiral derivatives of the stilbazole/iodostilbene

complexes, we extended the study to the preparation of chiral analogues by functionalising both components with chiral chains derived from citronellol. The *R* and *S* derivatives of each component were prepared and for each enantiomeric component, three complexes were prepared with three chain lengths of the complementary component (*m*, *n* = 4, 8, 12) and complexes were prepared in which both halves were chiral to give a family of sixteen new mesogens. The complexes were prepared by co-crystallisation of the two components from chloroform.

Complexes formed by the self-assembly of the stilbazole **1**-(*S*) with the fluorinated stilbenes **2**-4, **2**-8 and **2**-12 showed an enantiotropic N* mesophase (Figure 5) that exhibited a

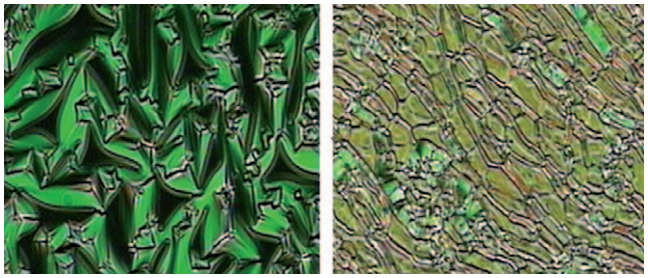

Figure 5. Optical texture of the phase transition of **1**-*S*·**2**-4 detected at the same temperature on cooling. Fan-like texture (left), oily streak texture after shearing (right).

typical focal conic fan texture, which is the main feature of N* chiral liquid crystals with short pitch length. This texture changed after shearing to give a planar texture with oily streaks. The liquid-crystalline range was 18.4 °C for **1**-(*S*)·**2**-4, a little higher than for the equivalent achiral complex bearing the same number of carbon atoms on the alkyl chain. However, this does not reflect the fact that both melting and clearing points are destabilised with respect to the achiral analogues owing to the presence of the doubly branched chain and unsaturated link, both of which are destabilising. The enantiomeric materials, **1**-(*R*)·**2**-*n* mirrored the transition temperatures of the *S* enantiomer almost precisely. The transition temperatures for all complexes are reported in Table 4.

We next prepared the analogous complexes (**1**-*m*·**2**-(*S*) and **1**-*m*·**2**-(*R*)) in which the chiral function was located on the iodostilbene. In this case we again found little difference between the transition temperatures of the two enantiomers and in fact the melting points of the *m* = 4 and 8 derivatives vary little between the four series examined. However, the difference lies with **1**-12·**2**-(*S*) and **1**-12·**2**-(*R*), which instead of showing a N* phase in fact formed a SmA* phase. This formed as a focal-conic texture and was distinguished from the N* phase by its behaviour on shearing. In this way, complex **1**-12·**2**-(*S*) (or its *R* enantiomer) more closely resembles the achiral analogues that showed a SmA phase when the stilbazole chain length was *m* = 12. Interestingly then, this implies that the stilbazole may have a slightly greater effect on the mesomorphism in these complexes.

Table 4. Thermal data for the chiral halogen-bonded complexes.

	Transition	*T* [°C]	Δ*H* [kJ mol^{-1}]
1-(*S*)·**2**-4	Cr–N*	73.8	43.4
	N*–I	92.2	5.5
1-(*R*)·**2**-4	Cr–N*	74.2	17.5
	N*–I	92.5	2.4
1-(*S*)·**2**-8	Cr–N*	75.5	36.2
	N*–I	84.5	3.1
1-(*R*)·**2**-8	Cr–N*	74.8	74.4
	N*–I	84.1	11.8
1-(*S*)·**2**-12	Cr–N*	86.9	49.9
	N*–I	91.7	4.9
1-(*R*)·**2**-12	Cr–N*	87.3	44.3
	N*–I	91.0	4.3
1-4·**2**-(*S*)	Cr–N*	74.0	5.3
	N*–I	95.4	0.9
1-4·**2**-(*R*)	Cr–N*	73.2	35.4
	N*–I	94.4	5.7
1-8·**2**-(*S*)	Cr–N*	75.3	22.1
	N*–I	93.3	2.0
1-8·**2**-(*R*)	Cr–N*	74.6	66.6
	N*–I	94.1	15.9
1-12·**2**-(*S*)	Cr-SmA*	81.5	14.9
	SmA*–I	94.5	6.7
1-12·**2**-(*R*)	Cr-SmA*	81.9	19.8
	SmA*–I	95.2	8.3
1-(*S*)·**2**-(*S*)	Cr–N*	65.0	51.9
	N*–I	69.5	7.1
1-(*S*)·**2**-(*R*)	Cr–N*	37.9	28.4
	N*–I	63.8	3.2
1-(*R*)·**2**-(*S*)	Cr–N*	38.4	27.5
	N*–I	64.2	3.0
1-(*R*)·**2**-(*R*)	Cr–N*	64.6	10.3
	N*–I	69.4	1.0

Complexes between stilbazoles (1-*m*) and alkoxytetrafluoroiodobenzenes (6-*n*): The majority of these complexes (Scheme 6) were prepared by crystallisation from a solution

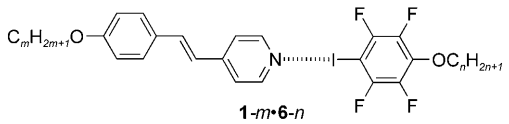

1-*m*•**6**-*n*

Scheme 6. General structure for complexes **1**-*m*·**6**-*n*.

of the two components in THF, but for some combinations (see Table 5) the crystallisation failed. In these cases, the complexes were prepared by weighing equimolar quantities of the two components and melting them together carefully. In order to assess the appropriateness of this approach, we re-prepared by this method some complexes that we could obtain by crystallisation and found that the mesophase seen was identical, although transition temperatures were between 1 and 3 °C lower. These results suggest that the method is adequate to enable a proper comparison to be made, although it does suggest that crystallisation is preferable where it works. The thermal data for these complexes are collected in Table 5.

Table 5. Thermal data for complexes between alkoxystilbazoles (**1**-*m*) and alkoxytetrafluoroiodobenzenes (**6**-*n*).

	Transition	T [°C]	ΔH [kJ mol^{-1}]
1-4·**6**-4	Cr–Iso	73.3	22.7
	(SmA–Iso)	(67.1)	(5.7)
1-4·**6**-6	Cr–SmA	64.5	19.5
	SmA–Iso	66.7	8.7
1-4·**6**-8	Cr–SmA	60.9	24.1
	SmA–Iso	65.0	9.8
1-4·**6**-10	Cr–SmA	53.9	27.9
	SmA–Iso	65.3	8.5
1-4·**6**-12	Cr–Iso	61.0	37.7
	(SmA–Iso)	(60.8)	(7.4)
1-6·**6**-4	Cr–SmA	66.7	26.0
	SmA–Iso	72.1	9.7
1-6·**6**-6	Cr–SmA	55.7	18.5
	SmA–Iso	70.4	11.2
1-6·**6**-8	Cr–SmA	66.6	28.8
	SmA–Iso	70.6	12.1
1-6·**6**-10	Cr–SmA	58.1	37.4
	SmA–Iso	68.3	10.6
1-6·**6**-12	Cr–SmA	60.4	47.6
	SmA–Iso	65.2	10.1
1-8·**6**-4	Cr–SmA	71.4	6.9
	SmA–Iso	77.0	13.6
1-8·**6**-6	Cr–SmA	57.4	19.5
	SmA–Iso	74.0	12.2
1-8·**6**-8	Cr–SmA	52.4	22.2
	SmA–Iso	75.0	14.0
1-8·**6**-10	Cr–SmA	58.5	43.8
	SmA–Iso	72.4	11.9
1-8·**6**-12	Cr–SmA	57.4	36.4
	SmA–Iso	72.8	14.4
1-10·**6**-4[a]	Cr–SmA	65.6	23.9
	SmA–Iso	79.3	14.3
1-10·**6**-6[a]	Cr–SmA	38.9	14.7
	SmA–Iso	78.3	9.8
1-10·**6**-8[a]	Cr–SmA	60.5	37.9
	SmA–Iso	77.5	26.8
1-10·**6**-10[a]	Cr–SmA	51.4	24.7
	SmA–Iso	73.4	15.0
1-10·**6**-12[a]	Cr–SmA	59.3	35.0
	SmA–Iso	73.3	13.8
1-12·**6**-4[a]	Cr–SmA	58.7	27.3
	SmA–Iso	79.5	16.6
1-12·**6**-6[a]	Cr–SmA	57.0	24.0
	SmA–Iso	76.9	15.6
1-12·**6**-8[a]	Cr–SmA	53.6	26.1
	SmA–Iso	76.4	18.7
1-12·**6**-10[a]	Cr–SmA	53.2	26.4
	SmA–Iso	75.9	17.3
1-12·**6**-12[a]	Cr–SmA	71.8	51.4
	SmA–Iso	77.3	19.8

[a] Complexes prepared by melting equimolar amounts of the components.

All of the complexes showed only a SmA phase, which was readily identified by the appearance of a focal conic fan texture and/or a homeotropic texture with oily streaks on shearing and for all but two complexes (**1**-4·**6**-4 and **1**-4·**6**-12), the mesophases were enantiotropic. The complexes showed a range of melting enthalpies, but clearing enthalpies varied from about 6 up to almost 27 kJ mol^{-1}. These higher values are rather surprising and are somewhat greater than would be expected for the clearing of a SmA phase. However, in previous papers[12b,c] we have noted the tendency for some complexes to exhibit partial dissociation when passing to the isotropic phase and we suspect that this is the case here, too.

In general, the transition temperatures for these complexes are rather low given their structure, which contains three aromatic rings. It would be expected that clearing points for such materials would be much higher and, for example, hydrogen-bonded complexes between alkoystilbazoles and 4-alkoxybenzoic acids typically give mesophases between 100 and 150 °C .[19] In turn, these are again lower than might be expected for covalent analogues due to the extra flexibility conferred by the hydrogen bond. The transition temperatures can again be plotted in two ways: one (shown in Figure 6) that shows how they depend on the stilbazole chain length and the other (see Supporting Information, Figure SI-2) that shows how they depend on the alkoxytetrafluoroiodobenzene chain length. What is interesting is that Figure 6 shows a clear dependence on the stilbazole chain length, while Figure SI-2 (Supporting Information) shows a rather small dependence on the iodobenzene chain length, with the clearing point decreasing slowly with increasing iodide chain length.

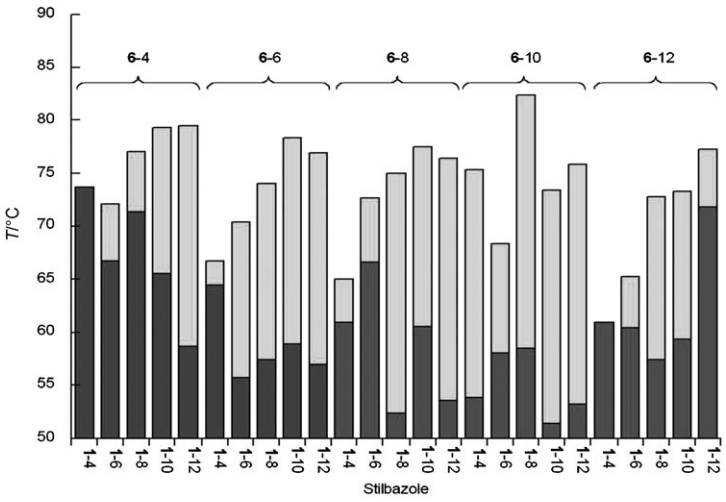

Figure 6. Plot of transition temperatures for complexes **1**-*m*·**6**-*n* as a function of stilbazole chain length (dark grey is crystal phase, light grey is SmA).

Complexes between stilbazoles (1-*m*) and the two-ring esters 3-*n*, 4-*n* and 5-*n*: Examination of the thermal data for these complexes (Scheme 7; Table 6) shows that the majority exhibit a monotropic mesophase, which is, for most complexes, nematic. However, again we note that the transition temperatures are significantly lower than one might expect for a complex that is so anisotropic, being composed of four aromatic rings. For example, the four-ring mesogen: $C_8H_{17}O$-Ph-CO_2-Ph-CH=N-Ph-O_2C-Ph-OC_8H_{17} shows N–Iso at 298 °C.[25] Another point worthy of note here is that it is possible to predict which of the esters should form the stron-

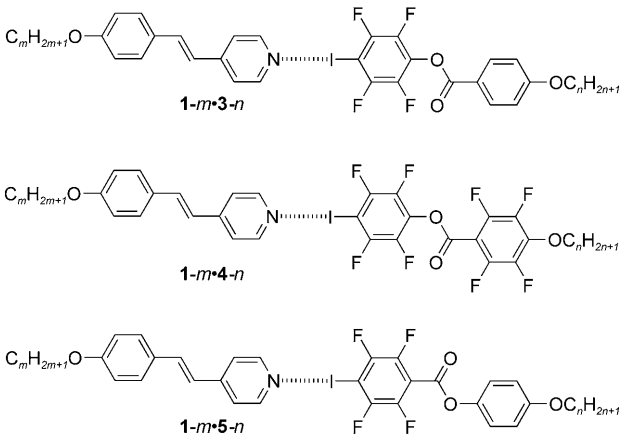

Scheme 7. General structures for complexes **1**-*m*·**3**-*n*, **1**-*m*·**4**-*n* and **1**-*m*·**5**-*n*.

Table 6. Thermal data for complexes (all prepared in the melt) between alkoxystilbazoles (**1**-*m*) and esters **3**-*n*, **4**-*n* and **5**-*n*.

	Transition	T [°C]	ΔH [kJ mol^{-1}]
1-6·**3**-6	Cr–Iso	135.5	63.6
	(N–Iso)	(102.5)	–
1-6·**3**-10	Cr–Iso	128.5	68.8
	(N–Iso)	(102.4)	–
1-10·**3**-6	Cr–Iso	129	69.3
1-10·**3**-10	Cr–Iso	127.8	74.3
1-4·**4**-6	Cr–N	85.5	20.1
	N–Iso	101.9	6.5
1-6·**4**-6	Cr–N	74.8	–
	N–Iso	86.7	–
1-6·**4**-10	Cr–N	87.9	40.0
	N–Iso	92.6	8.7
1-10·**4**-6	Cr–SmA	79.1	–
	SmA–N	82.6	–
	N–Iso	87.0	–
1-10·**4**-10	Cr–Iso	88.5	52.2
	(N–Iso)	(87.4)	–
1-12·**4**-6	Cr–Iso	98.7	34.6
	(N–Iso)	(95.4)	–
1-6·**5**-6	Cr–Iso	113.8	26.4
	(N–Iso)	(106.4)	–
1-6·**5**-**1**0	Cr–Iso	104.8	23.5
	(N–Iso)	(96.5)	–
1-10·**5**-6	Cr–Iso	108.0	19.6
	(SmA–Iso)	(93.0)	–
1-10·**5**-10	Cr–Iso	101.1	47.3
	(SmA–Iso)	(88.9)	–

gest halogen bonds with the stilbazoles, if it is assumed that the most δ^+ iodine will interact most strongly with the pyridine nitrogen. On this basis, we suggest that the order would be: **5**-n > **4**-n > **3**-n. If the clearing points of the different complexes are now considered (Figure 7), it is readily apparent that there is no systematic dependence of the clearing point on the type of ester, which suggests strongly that in this series, rupture of the halogen bond is not a significant factor in driving the clearing transition.

Complexes between octylpyridine(7) and the two-ring esters 3-*n*, 4-*n* and 5-*n* and iodostilbenes 2-*n*: In selecting to prepare these complexes (Scheme 8), we had identified a three-ring motif analogous to complexes **1**-*m*·**6**-*n*, except that it was the two-ring unit that carried the iodine. Most complexes showed monotropic nematic phases (Table 7), but what was remarkable was the extremely low transition temperatures for the complexes of the esters, so much so that the clearing points of **7**·**4**-6 and **7**·**4**-10 were sub-ambient, while that of **7**·**5**-6 was found at −9 °C. However, these com-

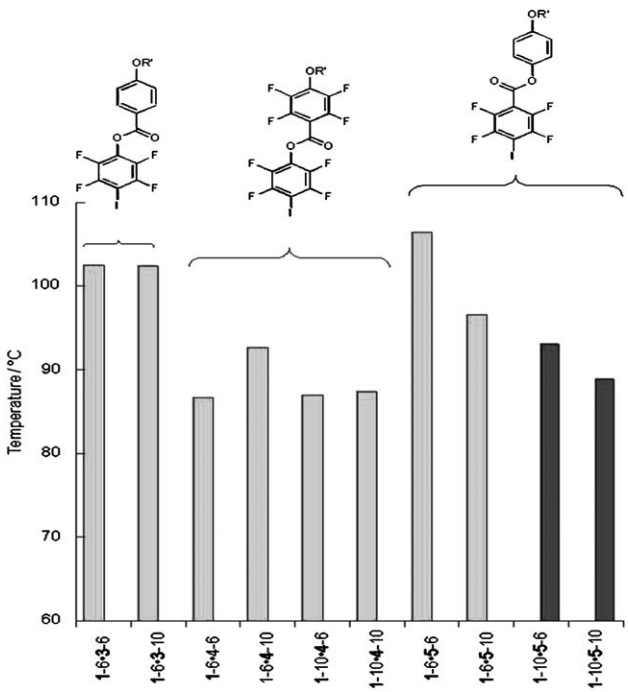

Figure 7. Plot of clearing points as a function of fluoroester and stilbazole chain length. Data in light grey refer to N–Iso, while those in dark grey refer to SmA–Iso.

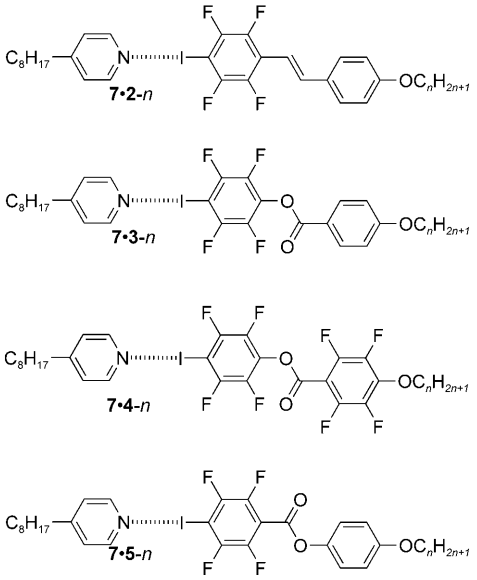

Scheme 8. General structures for complexes **7**·**2**-**5**-*n*.

Table 7. Thermal data for complexes between octylpyridine (**7**) and esters **3**-*n*, **4**-*n* and **5**-*n*.

	Transition	T [°C]	ΔH [kJ mol^{-1}]
7·**2**-6	Cr–N	57.2	–
	N–Iso	62.3	–
7·**2**-10	Cr–N	56.8	–
	N–Iso	61.5	–
7·**3**-6	Cr–Iso	39.1	56.2
	(N–Iso)	(23.8)	(4.7)
7·**3**-10	Cr–N	35.0	30.1
	N–Iso	36.7	5.9
7·4-6	Cr–Iso	42.1	32.9
	(N–Iso)	(13.0)	(2.4)
7·**4**-10	Cr–Iso	34.1	44.1
	(N–Iso)	(17.7)	(3.7)
7·**5**-6	Cr–Iso	25.6	13.5
	(N–Iso)	(−9.1)	–
7·**5**-10	Cr–Iso	61.4	35.3
	(N–Iso)	(13.0)	–

plexes do not make for a good comparison with the series **1**-*m*·**6**-*n*, as the former contain an ester function, which will tend to act to destabilise the mesophases. Thus it is complexes **7**·**2**-6 and **7**·**2**-10 that must be used. In both cases, an enantiotropic nematic phase was found and there was remarkably little difference between the transition temperatures of the two.

The phase behaviour of these two complexes can be compared with that of **1**-8·**6**-6, **1**-8·**6**-10, **1**-6·**6**-8 and **1**-10·**6**-8, for which the clearing point varies from 70.6 to 77.5 °C. Although the T_{NIso} values for these complexes are a little higher, they are no so different from those of **7**·**2**-6 and **7**·**2**-10, showing that the major factor determining the mesophase stability is the overall molecular composition.

While not wishing to extend this series too much further, we did prepare two examples of analogous complexes using 4-octyloxypyridine (Scheme 9), and these materials also

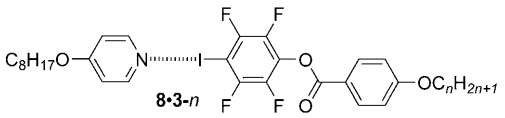

8•**3**-6: Cr (• N • 49.0) • 73.8 • Iso
8•**3**-10: Cr (• N 38.2) • 66.0 • Iso

Scheme 9. General structures for complexes **8**·**3**-*n*.

showed monotropic phases, but at appreciably higher transition temperatures. That these transition temperatures are higher is consistent with the stabilising effect of the ether oxygen.

However, having realised materials with rather low clearing points, we prepared one, final set of complexes between octyl- (or octyloxy-) pyridine and the alkoxyiodobenzenes **6**-*n*. Thus, as part of his work on hydrogen-bonded systems, Kato and co-workers had shown that complexes formed between these pyridines and alkoxybenzoic acids showed liquid-crystal phases at and around ambient temperature.[26] Therefore we prepared four complexes in which each of **7** and **8** was complexed to **6**-4 and **6**-10 (Scheme 10). None of these complexes was mesomorphic and all showed melting points below 0 °C.

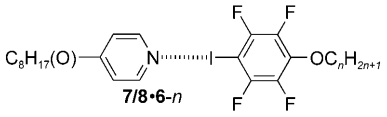

Scheme 10. General structures for complexes **7**/**8**·**6**-*n*.

Discussion

In the majority of cases reported in this paper, the complexes studied were prepared by co-crystallising the two components, which tended to lead to materials with sharp melting points; this remains the preferred method of preparation. However, in some cases such a co-crystallisation failed and so samples were prepared by melting together carefully weighed amounts of the two components. In control situations, comparison of transition temperatures with samples prepared by crystallisation gave very similar results indicating that melting the samples together is good enough to determine and compare mesomorphism. However, the fact that sharp melting was not observed shows that complex formation was not complete. This differs from our experience with hydrogen-bonded liquid crystals and is perhaps indicative of a possibly greater lability in these halogen-bonded systems.

One of the major observations is that the majority of the materials showed enantiotropic mesophases, something that was not a feature of several previous reports.[10,12a,b] The observation of a mesophase as monotropic or enantiotropic represents a balance between the melting point of the complex and the stability of its liquid-crystal phase and, compared to previous materials reported by us, it is the destabilisation of the crystal phase that accounts for the predominance of enantiotropic phases. It is possible to rationalise this behaviour. Thus, we have reported previously the phase behaviour of 2:1 complexes of alkoxystilbazoles with 1,4-diiodotetrafluorobenzene and found typically that the complexes melted (Cr–Iso) between 115–130 °C, with monotropic clearing points around 110–113 °C.[12b] In the present case, melting points for complexes **1**-*m*·**2**-*n* are mostly around 104–115 °C, whereas clearing points are between 110–120 °C. In comparing the two series, the 2:1 complexes of the diiodotetrafluorobenzene are more anisotropic, containing five rings and so it is perhaps not surprising that they melt at temperatures slightly higher than those found for **1**-*n*·**2**-*n*. In principle, this anisotropy ought also to be reflected in higher clearing points, but the fact that it is not points to an important aspect of the mesomorphism of moieties formed by non-covalent, monodentate interactions.

For example, in previous work with hydrogen-bonded mesogens (Scheme 11), an analogy was drawn between a pyridine hydrogen-bonded to a benzoic acid and a simple

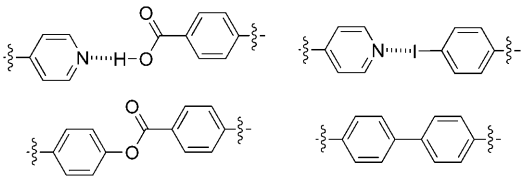

Scheme 11. General structures of hydrogen-bonded mesogens,[25] analogues of halogen-bonded mesogens.

ester.[27] Such an analogy allowed the effects of the flexibility of the hydrogen bond to be assessed and it was found to be substantial, reducing clearing points by comfortably in excess of 100 K. If a halogen bond is then considered as structurally similar to a σ-bond (a space-filling representation of **1**-10·**2**-6 shows that the size of the iodine is not an additional factor), then a search of the literature shows no directly analogous compounds for which liquid-crystal properties are reported. However, by comparing the clearing points of **1**-8·**2**-8 (114.6 °C) and the 2:1 complex of octyloxystilbazole with 1,4-diiodotetrafluorobenzene (113.5 °C)[12b] with those of the four-ring (**9**)[25] and five-ring (**10**)[28] compounds shown below (Scheme 12), some progress can be made.

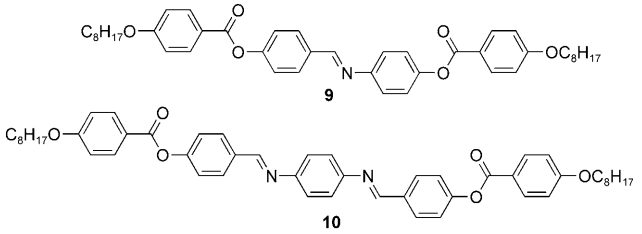

Scheme 12. Structures of liquid-crystalline materials with four (**9**) and five aromatic rings (**10**).

Thus, the clearing point of **9** is 298 °C, while that of **10** is at least 422 °C. Using these to compare with the halogen-bonded mesogens shows that one halogen bond can destabilise the clearing point by close to 200 °C, while two halogen bonds lead to a reduction of around 300 °C. It is possible that this last comparison represents an overestimate, as we argued that it was conceivable that, in contrast to the situation in hydrogen-bonded mesogens, the clearing points in the 2:1 complexes (with both 1,4- and 1,3-diiodotetrafluorobenzene) were limited by the stability of the halogen bond, as evidenced by the relatively insensitivity of the clearing point to chain length. However, complexes **1**-*n*·**2**-*n* do show sensitivity to chain length, suggesting that halogen-bond rupture does not drive the clearing behaviour and so the destabilisation of around 200 °C can be regarded as valid. Nonetheless, it is reasonable to assume that two halogen bonds will show a greater destabilisation. Thus, the fact that so many of the complexes studied show enantiotropic mesomorphism when compared to the previous 2:1 systems can be attributed to a significantly smaller mesophase destabilisation (only one halogen bond) accompanied by a destabilisation of the crystal phase owing to the reduced anisotropy of the complex.

Yet despite the fact that the presence of the halogen bond destabilises the clearing point, the complexes are otherwise rather insensitive to its presence. This is shown clearly by Figure 8 in which the clearing points for **1**-*m*·**2**-*n* are plotted

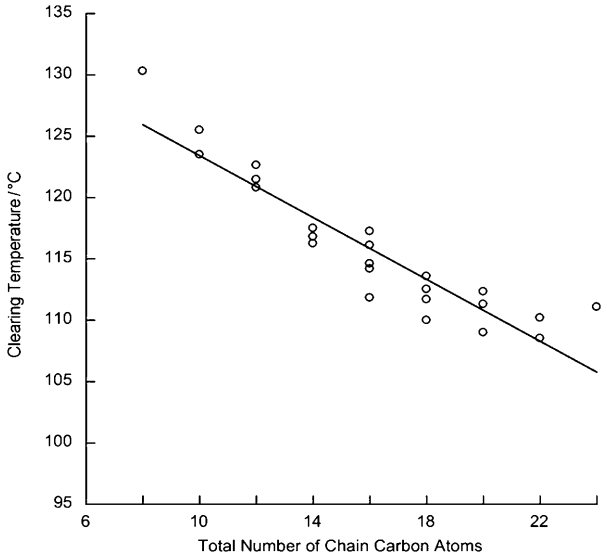

Figure 8. Clearing point as a function of total carbon chain length for complexes **1**-*m*·**2**-*n*.

as a function of the total chain length, indicating that the complexes do not discriminate between the positioning of the chains. This is supported by the observations with the chiral analogues, for which clearing points were also insensitive to the moiety bearing the chiral and the achiral chain. Furthermore, this monotonic increase with decreasing total chain length shown in Figure 8 argues that where there is a single halogen bond, mesophase stability does not appear to be limited by halogen bond strength at least to around 130 °C.

Finally, we note that in some series of materials, there is a pronounced dependence of the mesomorphic properties on the stilbazole, which is not mirrored as a function of the iodine acceptor. The reasons for this are not clear, but it is an observation that deserves mention given the data in Figure 8. It is to be expected that this point will addressed in due course through further study.

Conclusion

In reporting some ninety new complexes in this work, we present for the first time a substantial and systematic study

of halogen-bonded liquid crystals. Thus, the present study shows that halogen bonding may be used reliably for the construction of new, supramolecular mesogens and that at least in cases in which there is a single halogen bond present, mesophase stability is not limited by halogen-bond strength. Furthermore, general arguments that are used to account for the mesophase stability of covalent mesogens may also be used for halogen-bonded systems once allowance is made for the flexibility of the halogen bond. Of course, there remain many mesogenic systems that as yet have no analogy in halogen-bonded equivalents and only time will show if they are similarly well behaved. Nonetheless, the results of this systematic study present an optimistic prognosis.

Experimental Section

Materials and methods: Commercial HPLC-grade solvents were used without further purification. Starting materials were purchased from Sigma–Aldrich, Acros Organics, and Apollo Scientific. ^{1}H, ^{13}C and ^{19}F NMR spectra were recorded at ambient temperature with Bruker 250, 270, 400 and 500 MHz spectrometers. Unless otherwise stated, $CDCl_3$ was used as both solvent and internal standard in ^{1}H and ^{13}C NMR spectra. For ^{19}F NMR spectra, $CDCl_3$ was used as solvent and $CFCl_3$ as internal standard. All chemical shift values are given in ppm. The mass spectra were recorded on a GC-MS AGILENT GC-MSD5975. Differential scanning calorimetry (DSC) analysises were performed on a Mettler Toledo DSC823e and DSC822e instruments, aluminium light 20 μL sample pans and the Mettler: STARe software for calculation. Melting points were also determined Reichert instrument by observing the melting and crystallising process through an optical microscope.

Optical microscopy was performed using an Olympus BX50 microscope and Olympus BX51 at ×100 and ×200 magnification with a Linkam Scientific LTS 350 heating stage and VWR international 18×18 mm borosilicate glass microscope cover slips of a thickness no. 1. Optical rotations were measured on a Jasco DIP-181 polarimeter.

All synthetic details, NMR spectra, melting points and mass spectra for the synthesised compounds are reported in the Supporting Information.

General procedure for the formation of 3-[2-(4-alkyloxyphenyl)vinyl]-1,2,4,5-tetrafluorobenzene (2-SII) (Scheme 13): Phosphonium salt (2.57 mmol) and NaH (3.34 mmol) were stirred in DMF (5 mL) for 30 min. Then, the aldehyde (**2**-SI;[18] 4.95 mmol) was added to the mixture and the solution was heated to 40 °C. After 24 h, the reaction was poured on H_2O and a white solid was filtered. The residue was purified by flash chromatography on silica gel (240–400 mesh), eluent hexane/CH_2Cl_2 (5:1), to give the products as solid powder (yield 73% for **2**-SII-butyl; 62% for **2**-SII-hexyl; 85% for **2**-SII-octyl; 95% for **2**-SII-decyl; 81% for **2**-SII-dodecyl; 51% for **2**-SII-*R*-citronellyl and 59% for **2**-SII-*S*-citronellyl).

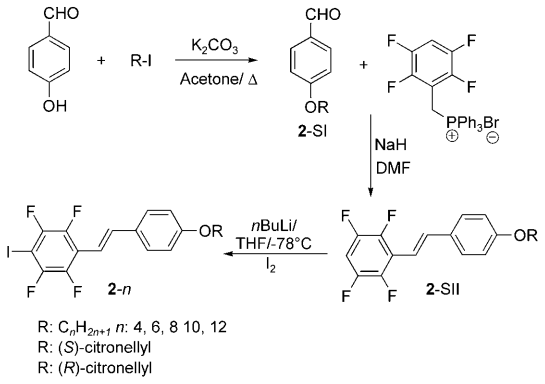

Scheme 13. Synthetic scheme for compounds **2**-*n*.

General procedure for the formation of 1-[2-(4-alkyloxyphenyl)vinyl]-2,3,5,6-tetrafluoro-4-iodobenzene (2-*n*): The fluorinated derivative (**2**-SII; 1.54 mmol) was stirred in suspension in THF (5 mL) at −78 °C. *n*BuLi (1.4 M, 2.31 mmol) was added slowly and the mixture was warmed up to room temperature. After 20 min, I_2 (2.31 mmol) was added and the solution was mixed 25 min. Then, the reaction was hydrolysed with $Na_2S_2O_3$ sat., the aqueous layer was extracted three times with CH_2Cl_2 and the organic phase was dried over anhydrous Na_2SO_4. After evaporation of the solvent, the compound **2**-*n* was recovered in pure form without further purification (yield 95% for **2**-4; 90% for **2**-6; 85% for **2**-8; 95% for **2**-10; 81% for **2**-12; 79% for **2**-(*R*) and 90% for **2**-(*S*)).

General procedure for the formation of 4-iodo-2,3,5,6-tetrafluorophenol (3-SI) (Scheme 14): Pentafluoroiodobenzene (34 mmol) with KOH (102 mmol) was heated under reflux in *tert*-butyl alcohol (30 mL) for 6.5 h (oil bath heated to 90 °C). Aqueous hydrochloric acid (5%, 20 mL) was added and the aqueous *tert*-butyl alcohol was distilled off under vacuum. The residue was acidified to ≈pH 2 with aqueous hydrochloric acid (5%). The filtrate was extracted with ether and dried over anhydrous Na_2SO_4. The solvent was removed by rotary evaporation and the white solid collected (60% yield).[29]

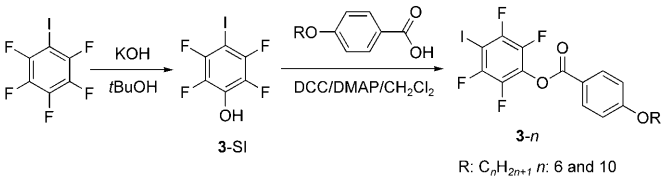

Scheme 14. Synthetic scheme for compounds **3**-*n*.

General procedure for the formation of 4-(4-alkoxyphenyl)-2,3,5,6-tetrafluoroiodobenzoate (3-*n*): Compound **3**-SI (6.8 mmol), 4-alkyloxybenzoic acid (6.8 mmol), 1,3-dicyclohexylcarbodiimide (7.5 mmol) and 4-(*N*,*N*-dimethylamino)pyridine (0.3 mmol) were placed in a round-bottomed flask with dry dichloromethane (50 mL) and stirred for 48 h at room temperature. The white precipitate was filtered off and the filtrate was washed with aqueous acetic acid (5%, 100 mL). The organic layer was separated; the solvent removed by rotary evaporation and the pale yellow solid was collected. The crude product was re-dissolved in pentane and ethyl acetate (30:1) and passed through a silica flash chromatography column. The solvent was then removed by rotary evaporation and the white powder was collected (yield 59% for **3**-6 and 8% for **3**-10).

General procedure for the formation of 4-(4-alkoxy-2,3,5,6-tetrafluorobenzoyloxy)-2,3,5,6-tetrafluoroiodobenzenes (4-SII) (Scheme 15): 2,3,5,6-Tetrafluorophenol (24 mmol), anhydrous potassium carbonate (29 mmol) and acetonitrile (40 mL) were placed in a round-bottomed flask fitted with a reflux condenser, nitrogen inlet and magnetic stirrer. The reaction mixture was heated to reflux (oil bath heated to 85 °C) and stirred. Once reflux was reached, 1-bromoalkane (23 mmol) was added dropwise over 10 min. The mixture was heated under reflux for 12 h before cooling. Once the mixture had cooled to room temperature, it was treated with water (100 mL) and extracted with petroleum ether (50 mL). The organic layer was then washed with NaOH (10%, 2×50 mL each) and finally with water until neutrality was reached. The organic solution was dried over anhydrous Na_2SO_4 and the solvent removed using rotary evaporation leaving a pale yellow oil, no further purification was carried out (yield 97% for **4**-SI-hexyl and 79% for 4-SI-decyl). *n*-Butyl lithium (2.5 M in hexane, 10 mmol) was cooled in an acetone/dry ice bath (−70 °C) in dried glassware. Dry THF (20 mL) and diisopropylamine (10 mmol) were added and allowed to cool. Compound **4**-SI (10 mmol) in dry THF (10 mL) was added drop-wise over 5 min. The reaction was left to stir (at −70 °C) for 30 min. CO_2 was then bubbled through the mixture and it

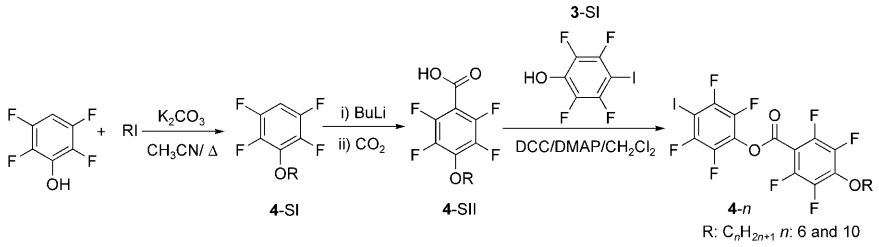

Scheme 15. Synthetic scheme for compounds **4**-*n*.

was slowly allowed to return to room temperature. The solvent was removed by vacuum and the crude product treated with water (30 mL) and HCl (1 M) to bring the pH to ≈2. The product was extracted with diethyl ether, which was then removed by rotary evaporation to leave a white solid (yield 51% for **4**-SII-hexyl and 45% for **4**-SII-decyl) .[30]

General procedure for the formation of 4-(4-alkyloxy-2,3,5,6-tetrafluorobenzoyloxy)-2,3,5,6-tetrafluoroiodobenzenes (4-*n*): Compound (**4**-SII) (5.1 mmol), 1,3-dicyclohexylcarbodiimide (5.6 mmol) and 4-dimethylaminopyridine (0.2 mmol) were used in the same method described in the preparation of **3**-*n* compounds and the white powder was collected (yield 51% for **4**-6 and 45% for **4**-10).

General procedure for the formation of 4-(4-alkoxybenzoyloxy)-2,3,5,6-tetrafluoroiodobenzenes (5-SI) (Scheme 16): Pentafluorobenzoic acid (48 mmol), zinc powder (0.19 mol) and 20% aqueous ammonia solution

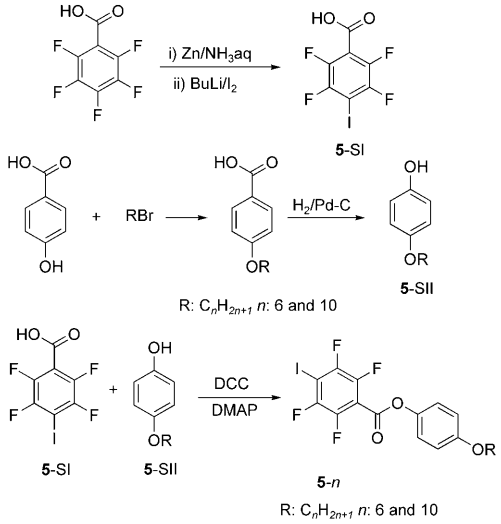

Scheme 16. Synthetic scheme for compounds **5**-*n*.

(90 mL) were stirred at room temperature for 24 h. The zinc was removed and the remaining solution acidified with HCl. The product was extracted with diethyl ether which was later removed by rotary evaporation and the intermediate collected. 2,3,5,6-Tetrafluorobenzoic acid (27 mmol) was treated with *n*BuLi (2.5 M in hexane, 53 mmol) and iodine added (26 mmol) using the same procedure reported for the preparation of **6**-*n* (yield 59% for **5**-SI) .[31]

General procedure for the formation of 4-alkyloxyphenol (5-SII): Small pieces of metallic sodium (10 mmol) were carefully dissolved in ethanol (20 mL). To this 4-benzyloxyphenol (9 mmol) and 1-bromoalkane (10 mmol) were added and the mixture was heated under reflux for 24 h (85 °C). The mixture was cooled and the NaBr formed was removed by filtration and washed with dichloromethane. The solvent was then removed by rotary evaporation. The crude product was re-dissolved in chloroform and washed with water (50 mL), HCl (1 M) and again with water until neutral. The intermediate (3 mmol) was dissolved in ethanol (20 mL) and Pd/C was added and stirred vigorously under hydrogen for 24 h. The catalyst was filtered off, washed with dichloromethane and solvent removed by rotary evaporation and the products collected (yield 24% for **5**-SII-hexyl and 60% for **5**-SII-decyl over two steps).

General procedure for the formation of 4-(4-alkyloxybenzoyloxy)-2,3,5,6-tetrafluoroiodobenzenes (5-*n*): Compounds **5**-SI (1.5 mmol) and **5**-SII (1.5 mmol), 1,3-dicyclohexylcarbodiimide (1.7 mmol) and 4-(*N*,*N*-dimethylamino)pyridine (0.07 mmol) were used in the same method described in the preparation of **3**-*n* and the white powder was collected (yield 79% for **5**-6 and 71% for **5**-10).

General procedure for the formation of 4-alkoxy-2,3,5,6-tetrafluorobenzenes (6-SI) (Scheme 17): 2,3,5,6-Tetrafluorophenol (24 mmol), anhydrous potassium carbonate (29 mmol) and acetonitrile (40 mL) were

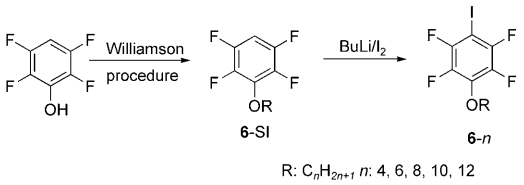

Scheme 17. Synthetic scheme for compounds **6**-*n*.

placed in a round-bottomed flask fitted with a reflux condenser, nitrogen inlet and magnetic stirrer. The reaction mixture was heated to reflux (85 °C) and stirred. Once reflux was reached, 1-bromoalkane (23 mmol) was added dropwise over 10 min. The mixture was heated under reflux for 12 h before cooling. Once the mixture had cooled to room temperature, it was transferred to a separating funnel, treated with water (100 mL) and extracted with petroleum ether (50 mL). The organic layer was then washed with NaOH (10%, 50 mL each) and finally with water until neutrality was reached. The organic solution was dried over anhydrous Na_2SO_4 and the solvent removed using rotary evaporation leaving a pale yellow oil, no further purification was carried out. (yield 95% for **6**-SI-butyl, 97% for **6**-SI-hexyl, 79% for **6**-SI-octyl, 79% for **6**-SI-decyl and 93% for **6**-SI-dodecyl).

General procedure for the formation of 4-alkoxy-2,3,5,6-tetrafluoroiodobenzenes (6-*n*): Anhydrous THF (20 mL) and compound **6**-SI (19 mmol) were cooled to −70 °C in dried glassware. *n*BuLi (2.5 M in hexane, 29 mmol) was added drop wise over 15 min and left to stir for a further 15 min at −70 °C. Iodine (29 mmol) dissolved in anhydrous THF (20 mL) was then slowly added to the reaction mixture until the colour remained brown. This was then allowed to slowly warm up to room temperature, while stirring. $H_2SO_{4(aq)}$ (20 mL) and water (30 mL) were then added and the aqueous phase was extracted with diethyl ether (50 mL). The organic layer was then washed with water (50 mL), once with $Na_2S_2O_{3(aq)}$ (50 mL) and then again with water before being dried over $MgSO_4$. The solvent was removed using rotary evaporation and the residue passed through silica with petroleum ether, which was then removed by rotary evaporation to leave colourless oil (yield 40% for **6**-4, 55% for **6**-6, 52% for **6**-8, 53% for **6**-10 and 18% for **6**-12).

Synthesis of 7: *n*BuLi (2.5 M in hexane, 70 mmol) was added drop wise to diisopropylamine (70 mmol) in dry THF (20 mL) in dried glassware under nitrogen, placed in a dry ice/ethanol bath (−70 °C) and allowed to stir for 30 min. This was then allowed to warm to −30 °C and the 4-methylpyridine (70 mmol) was slowly added and stirred for 1 h. 1-Bromoheptane

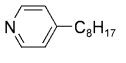

(70 mmol) was then added slowly to the reaction mixture and then stirred for a further hour. The mixture was allowed to return to room temperature and stirred for 48 h before quenching with water. The product was extracted with petroleum ether and dried over $MgSO_4$ before removing the solvent by rotary evaporation. The crude product was then distilled (at 159 °C) and the pure compound collected (32 % yield).[32]

Analysis by X-ray diffraction: The **1**·10·**2**·6 single-crystal X-ray structure was collected at 295(3) K with a Bruker KAPPA APEX II with CCDC area detector diffractometer using graphite-monochromated $Mo_{K\alpha}$ radiation ($\lambda = 0.71069$ Å); ω and ϕ scans; data collection and data reduction were performed with the SMART and SAINT program packages. The **1**·6·**6**·6 single crystal X-ray structure was determined at 110(3) K using a Bruker SMART-APEX diffractometer equipped with CCDC area detector using graphite-monochromated $Mo_{K\alpha}$ radiation ($\lambda = 0.71069$ Å); ω and ϕ scans; data collection and data reduction were performed with the SMART and SAINT program packages. The structures were solved by SIR2002[33] and refined by SHELXL-97[34] programs for **1**·10·**2**·6 and using SHELXS-97[34] and refined with SHELXL-97[34] for **1**·6·**6**·6. The refinement was carried on by full-matrix least-squares on F^2. Hydrogen atoms were placed using standard geometric models and with their thermal parameters riding on those of their parent atoms.

CCDC-769517 (**1**·10·**2**·6) and 769518 (**1**·6·**6**·6) contain the supplementary crystallographic data for this paper. These data can be obtained free of charge from The Cambridge Crystallographic Data Centre via www.ccdc.cam.ac.uk/data_request/cif.

Acknowledgements

We would like to thank Fondazione Cariplo (Project: New-Generation Fluorinated Materials as Smart Reporter Agents in ^{19}F MRI) and EPSRC for financial support and the Royal Society for a Joint Project Grant between the York and Milan laboratories.

[1] a) *Philos. Trans. R. Soc. A* **2006**, *364*, 2567–2843, edited by D. W. Bruce, H. J. Coles, J. R. Sambles; b) J. W. Goodby, *Chem. Soc. Rev.* **2007**, *36*, 1845–2128; c) C. Tschierske, *J. Mater. Chem.* **2008**, *18*, 2857–3060; d) T. Kato in *Handbook of Liquid Crystals* (Eds.: D. Demus, J. W. Goodby, G. W. Gray, H.-W. Spiess, V. Vill), Wiley-VCH, Weinheim, **1998**; e) *Thermotropic Liquid Crystals* (Ed.: G. W. Gray), Wiley, New York, **1987**; f) N. A. Platé, V. P. Shibaev, *Comb-Shaped Polymers and Liquid Crystals*, Plenum Press, New York, **1987**; g) U. Kumar, T. Kato, J. Fréchet, *J. Am. Chem. Soc.* **1992**, *114*, 6630–6631; h) T. Kato, Y. Kubota, T. Urya, S. Ujiie, *Angew. Chem.* **1997**, *109*, 1687–1689; *Angew. Chem. Int. Ed. Engl.* **1997**, *36*, 1617–1618.

[2] a) C. Dai, P. Nguyen, T. B. Marder, A. J. Scott, W. Clegg, C. Viney, *Chem. Commun.* **1999**, 2493–2496; b) N. Boden, R. J. Bushby, Z. Lu, O. R. Lozman, *Liq. Cryst.* **2001**, *5*, 657–661; c) N. Boden, R. J. Bushby, Z. Lu, O. R. Lozman, *J. Mater. Chem.* **2001**, *11*, 1612–1617; d) N. Boden, R. J. Bushby, G. Cooke, O. R. Lozman, Z. Lu, *J. Am. Chem. Soc.* **2001**, *123*, 7915–7916; e) K. Praefcke, J. D. Holbrey, *J. Inclusion Phenom. Mol. Recognit. Chem.* **1996**, *24*, 19–41; f) T. Hegmann, J. Kain, S. Diele, G. Pelzl, C. Tschierske, *Angew. Chem.* **2001**, *113*, 911–914; *Angew. Chem. Int. Ed.* **2001**, *40*, 887–890; g) C. Paleos, D. Tsiourvas, *Angew. Chem.* **1995**, *107*, 1839–1855; *Angew. Chem. Int. Ed. Engl.* **1995**, *34*, 1696–1711; h) T. Kato in *Handbook of Liquid Crystals, Vol. 2B* (Eds.. D. Demus, J. Goodby, G. W. Gray, H.-W. Spiess, V. Vill), **1998**, Wiley-VCH, Weinheim, Chapter XVII.

[3] a) F. Guthrie, *J. Chem. Soc.* **1863**, *16*, 239–244; b) I. Remsen, J. F. Norris, *Am. Chem. J.* **1896**, *18*, 90–95; c) O. Hassel, C. Rømming, *Q. Rev. Chem. Soc.* **1962**, *16*, 1–34; d) O. Hassel, *Science* **1970**, *170*, 497–502; e) A. C. Legon, *Angew. Chem.* **1999**, *111*, 2850–2880; *Angew. Chem. Int. Ed.* **1999**, *38*, 2686–2714; f) A. C. Legon, *Struct. Bonding* **2008**, *126*, 17–64; g) P. Metrangolo, G. Resnati, *Chem. Eur. J.* **2001**, *7*, 2511–2519; h) P. Metrangolo, G. Resnati in *Encyclopedia of Supramolecular Chemistry*, Marcel Dekker, New York, **2004**; i) P. Metrangolo, H. Neukirch, T. Pilati, G. Resnati, *Acc. Chem. Res.* **2005**, *38*, 386–395; j) P. Metrangolo, G. Resnati, T. Pilati, R. Liantonio, F. Meyer, *J. Polym. Sci. Part A* **2007**, *45*, 1–15; k) P. Metrangolo, T. Pilati, G. Resnati, A. Stevenazzi, *Curr. Opin. Colloid Interface Sci.* **2003**, *8*, 215–222; l) M. Formigué, *Curr. Opin. Chem. Biol.* **2009**, *13*, 36–45; m) K. Rissanen, *CrystEngComm* **2008**, *10*, 1107–1113; n) M. Baldrighi, P. Metrangolo, F. Meyer, T. Pilati, D. Proserpio, G. Resnati, G. Terraneo, *J. Fluorine Chem.* **2010**, DOI: 10.1016/j.jfluchem.2010.06.001; o) G. Cavallo, S. Biella, J. Lü, P. Metrangolo, T. Pilati, G. Resnati, G. Terraneo, *J. Fluorine Chem.* **2010**, DOI: 10.1016/j.jfluchem.2010.05.004; p) A. C. Legon, *Phys. Chem. Chem. Phys.* **2010**, *12*, 7736–7747; q) P. Politzer, J. S. Murray, T. Clark, *Phys. Chem. Chem. Phys.* **2010**, *12*, 7748–7757.

[4] a) P. Metrangolo, G. Resnati, *Science* **2008**, *321*, 918; b) P. Metrangolo, F. Meyer, T. Pilati, G. Resnati, G. Terraneo, *Angew. Chem.* **2008**, *120*, 6206–6220; *Angew. Chem. Int. Ed.* **2008**, *47*, 6114–6127; c) G. Cavallo, P. Metrangolo, T. Pilati, G. Resnati, M. Sansotera, G. Terraneo, *Chem. Soc. Rev.* **2010**, DOI:10.1039/b926232f.

[5] a) G. Marras, P. Metrangolo, F. Meyer, T. Pilati, G. Resnati, A. Vij, *New J. Chem.* **2006**, *30*, 1397–1402; b) T. Caronna, R. Liantonio, T. A. Logothetis, P. Metrangolo, T. Pilati, G. Resnati, *J. Am. Chem. Soc.* **2004**, *126*, 4500–4501; c) A. Sun, N. S. Goroff, J. W. Lauher, *Science* **2006**, *312*, 1030–1034.

[6] a) E. Cariati, A. Forni, S. Biella, P. Metrangolo, F. Meyer, G. Resnati, S. Righetto, E. Tordin, R. Ugo, *Chem. Commun.* **2007**, 2590–2592; b) J. Hulliger, P. J. Langley, *Chem. Commun.* **1998**, 2557–2558; c) J. A. R. P. Sarma, F. H. Allen, V. J. Hoy, J. A. K. Howard, R. Thaimattam, K. Biradha, G. R Desiraju, *Chem. Commun.* **1997**, 101–102; d) P. K. Thallapally, G. R. Desiraju, M. Bagieu-Beucher, R. Masse, C. Bourgogne, J. F. Nicoud, *Chem. Commun.* **2002**, 1052–1053.

[7] a) R. Bertani, P. Metrangolo, A. Moiana, E. Perez, T. Pilati, G. Resnati, I. Rico-Lattes, A. Sassi, *Adv. Mater.* **2002**, *14*, 1197–1201; b) F. Wang, N. Ma, Q. Chen, W. Wang, L. Wang, *Langmuir* **2007**, *23*, 9540–9542.

[8] a) P. Metrangolo, Y. Carcenac, M. Lahtinen, T. Pilati, K. Rissanen, A. Vij, G. Resnati, *Science* **2009**, *323*, 1461–1464.

[9] a) E. Guido, P. Metrangolo, W. Panzeri, T. Pilati, G. Resnati, M. Ursini, T. A. Logothetis, *J. Fluorine Chem.* **2005**, *126*, 197–207; b) P. Metrangolo, F. Meyer, T. Pilati, D. M. Proserpio, G. Resnati, *Chem. Eur. J.* **2007**, *13*, 5765–5772; c) P. Metrangolo, F. Meyer, T. Pilati, G. Resnati, G. Terraneo, *Chem. Commun.* **2008**, 1635–1637.

[10] H. L. Nguyen, P. N. Horton, M. B. Hursthouse, A. C. Legon, D. W. Bruce, *J. Am. Chem. Soc.* **2004**, *126*, 16–17.

[11] a) J. Xu, X. Liu, T. Lin, J. Huang, C. He, *Macromolecules* **2005**, *38*, 3554–3557; b) J. Xu, X. Liu, J. Kok-Peng, T. Lin, J. Huang, C. He, *J. Mater. Chem.* **2006**, *16*, 3540–3545.

[12] a) P. Metrangolo, C. Präsang, G. Resnati, R. Liantonio, A. C. Whitwood, D. W. Bruce, *Chem. Commun.* **2006**, 3290–3292; b) D. W. Bruce, P. Metrangolo, F. Meyer, C. Präsang, G. Resnati; G. Terraneo, A. C. Whitwood, *New J. Chem.* **2008**, *32*, 477–482; G. Terraneo, A. C. Whitwood, *New J. Chem.* **2008**, *32*, 477–482; c) C. Präsang, H. L. Nguyen, P. N. Horton, A. C. Whitwood, D. W. Bruce, *Chem. Commun.* **2008**, 6164–6166.

[13] C. Präsang, A. C. Whitwood, D. W. Bruce, *Chem. Commun.* **2008**, 2137–2139.

[14] a) D. S. L. Slinn, S. W. Green in *Preparation, Properties and Industrial Applications of Organofluorine Compounds* (Ed.: : R. E. Banks), Ellis Horwood, Chichester, **1982**, p. 45–82; b) G. Sandford, *Tetrahedron* **2003**, *59*, 437–454 and references therein; c) Z. Luo, Q. Zhang, Y. Oderaotoshi, D. P. Curran, *Science* **2001**, *291*, 1766–1769; d) I. Viola, G. Ciccarella, P. Metrangolo, G. Resnati, R. Cingolani, G. Gigli, *J. Fluorine Chem.* **2007**, *128*, 1335–1339.

[15] a) P. Kirsch, M. Bremer, *Angew. Chem.* **2000**, *112*, 4384–4405; *Angew. Chem. Int. Ed.* **2000**, *39*, 4216–4235; b) M. Hird, *Chem. Soc. Rev.* **2007**, *36*, 2070–2095; c) M. Hird, K. J. Toyne, *Mol. Cryst. Liq. Cryst.* **1998**, *323*, 1–67; d) F. Guittard, E. Taffin de Givenchy, S. Geribaldi, A. Cambon, *J. Fluorine Chem.* **1999**, *100*, 95–99; e) G. W. Gray, M. Hird, K. J. Toyne, *Mol. Cryst. Liq. Cryst.* **1991**, *204*, 43–64.

[16] M. P. Krafft, J. G. Riess, *Chem. Rev.* **2009**, *109*, 1714–1792.
[17] a) M. Yano, T. Taketsugu, K. Hori, H. Okamoto, S. Takenaka, *Chem. Eur. J.* **2004**, *10*, 3991–3999, and references therein; b) F. Tournilhac, L. M. Blinov, J. Simon, S. V. Yablonsky, *Nature* **1992**, *359*, 621–623; c) M. A. Guillevic, D. W. Bruce, *Liq. Cryst.* **2000**, *27*, 153–156; d) M. A. Guillevic, T. Gelbrich, M. B. Hursthouse, D. W. Bruce, *Mol. Cryst. Liq. Cryst.* **2001**, *362*, 147–170; e) L. Omnès, B. A. Timimi, T. Gelbrich, M. B. Hursthouse, G. R. Luckhurst, D. W. Bruce, *Chem. Commun.* **2001**, 2248–2249; f) L. Omnès, V. Cîrcu, P. T. Hutchins, S. J. Coles, M. B. Hursthouse, D. W. Bruce, *Liq. Cryst.* **2005**, *32*, 1437–1447; g) Y. Sasada, H. Monobe, Y. Ueda, Y. Shimizu, *Chem. Commun.* **2008**, 1452–1454.
[18] D. W. Bruce, D. A. Dunmur, E. Lalinde, P. M. Maitlis, P. Styring, *Liq. Cryst.* **1988**, 385–395.
[19] D. W. Bruce, *Adv. Inorg. Chem.* **2001**, *52*, 151–204.
[20] a) H.-C. Lin, J.-M. Shiaw, C.-Y. Wu, C. Tsai, *Liq.Cryst.* **2000**, *27*, 1103–1112; b) H.-C. Lin, J.-M. Shiaw, C.-Y. Wu, C. Tsai, *Liq. Cryst.* **1998**, *25*, 277–283.
[21] http://www.webelements.com/index.html, for van der Waals radii.
[22] S. V. Rosokha, I. S. Neretin, T. Y. Rosokha, J. Hecht, J. K. Kochi, *Heteroat. Chem.* **2006**, *17*, 449–459.
[23] Selected references: a) V. R. Thalladi, H.-C. Weiss, D. Bläser, R. Boese, A. Nangia, G. R. Desiraju, *J. Am. Chem. Soc.* **1998**, *120*, 8702–8710; b) N. N. L. Madhavi, G. R. Desiraju, C. Bilton, J. A. K. Howard, F. H. Allen, *Acta Crystallogr. Sect. A* **2000**, *56*, 1063–1070; c) G. R. Desiraju, *Acc. Chem. Res.* **2002**, *35*, 565–573; d) A. J. Mountford, D. L. Hughes, S. J. Lancaster, *Chem. Commun.* **2003**, 2148–2149; e) C. Li, S.-F. Ren, J.-L. Hou, H.-P. Yi, S.-Z. Zhu, X.-K. Jiang, Z.-T. Li, *Angew. Chem.* **2005**, *117*, 5871; *Angew. Chem. Int. Ed.* **2005**, *44*, 5725- 5729; f) D. Chopra, T. S. Cameron, J. D. Ferrara, T. N. Guru Row, *J. Phys. Chem. A* **2006**, *110*, 10465–10477; g) B. Bernet, A. Vasella, *Helv. Chim. Acta* **2007**, *90*, 1874–1888; h) N. Borho, Y. Xu, *J. Am. Chem. Soc.* **2008**, *130*, 5916–5921.
[24] K. Willis, J. E. Luckhurst, D. J. Price, J. M. J. Fréchet, T. Kato, G. Ungar, D. W. Bruce, *Liq. Cryst.* **1996**, *21*, 585–587.
[25] D. W. Bruce, X.-H. Liu, *J. Chem. Soc. Chem. Commun.* **1994**, 729–730.
[26] M. Fukumasa, T. Kato, T. Uryu, J. M. J. Fréchet, *Chem. Lett.* **1993**, 65–68.
[27] D. J. Price, H. Adams, D. W. Bruce, *Mol. Cryst. Liq. Cryst.* **1996**, *289*, 127–140.
[28] M.-A. Guillevic, M. E. Light, S. J. Coles, T. Gelbrich, M. B. Hursthouse, D. W. Bruce, *J. Chem. Soc. Dalton Trans.* **2000**, 1437–1445.
[29] J. Wen, H. Yu and Q. Chen, *J. Mater. Chem.* **1994**, *4*, 1715–1717.
[30] Y. Sasada, H. Monobe, Y. Ueda, Y. Shimizu, *Mol. Cryst. Liq. Cryst.* **2009**, *509* 928–936.
[31] a) T. Takeuchi, Y. Minato, M. Takase, H. Shinmori, Hideyuki, *Tetrahedron Lett.* **2005**, *46*, 9025–9027; b) C. B. Aakeroy, N. C. Schultheiss, A. Rajbanshi, J. Desper, C. Moore, *Cryst. Growth Des.* **2009**, *9*, 432–441.
[32] G. Viscardi, P. Savarino, P. Quagliotto, E. Barni, M. Botta, *J. Heterocycl. Chem.* **1996**, *33*, 1195–1200.
[33] M. C. Burla, M. Camalli, B. Carrozzini, G. L. Cascarano, C. Giacovazzo, G. Polidori, R. Spagna, *J. Appl. Cryst.* **2003**, *36*, 1103–1112.
[34] G. M. Sheldrick, *Acta Cryst.* **2008**, *A 64*, 112–122.

Received: March 22, 2010
Published online: July 21, 2010

